Λ-hypernuclear binding energy test of the refit Nijmegen soft core *YN* potential

Dean Halderson
Physics Department, Western Michigan University, Kalamazoo, Michigan 49001
(Received 23 August 1999; published 11 February 2000)

First order Brueckner-Hartree calculations for the Λ single-particle energies were performed with potentials Ib and IIa from a recent fit of the Nijmegen soft core potential parameters. The method was applied to ${}^{5}_{\Lambda}$He, ${}^{13}_{\Lambda}$C, ${}^{17}_{\Lambda}$O, ${}^{41}_{\Lambda}$Ca, ${}^{49}_{\Lambda}$Ca, ${}^{91}_{\Lambda}$Zr, and ${}^{208}_{\Lambda}$Pb. Although potentials Ib and IIa have very different short range characteristics, their results differed little over the $A=5$ to 209 mass range. The results for ${}^{5}_{\Lambda}$He and ${}^{17}_{\Lambda}$O$(1/2^{+},1/2^{-},3/2^{-})$ were within 0.7 MeV of the approximate calculations used in the fitting process. This shows that the inclusion of the approximate calculations in potential fits will provide reliable constraints. The $0p$-shell hypernuclei were in good agreement with experimental results, however, ${}^{5}_{\Lambda}$He was underbound by 0.9 and 1.0 MeV for the two potentials. It is emphasized that *g*-matrix procedures more suited for the heavy systems should be developed to have reliable predictions of hypernuclear saturation properties.

PACS number(s): 21.80.+a, 13.75.Jz, 21.10.Dr, 21.30.Fe

I. INTRODUCTION

The quest for a universal *YN* potential continues to be thwarted by the lack of scattering data. Particularly confounding is the lack of spin-dependent information. Consequently, potentials with vastly different spin and channel-coupling characteristics provide equally good fits to the existing scattering data. In an effort to alleviate some of this difficulty, four *BB* potentials have recently been developed in Ref. [1] with the Nijmegen soft core (NSC) formalism [2,3] by fitting selected bound state data as well as the traditional *YN* scattering data. The bound state data included were the ${}^{3}_{\Lambda}$H, ${}^{4}_{\Lambda}$H$(0^{+},1^{+})$, ${}^{5}_{\Lambda}$He, ${}^{17}_{\Lambda}$O$(1/2^{+},1/2^{-},3/2^{-})\Lambda$ separation energies and the ΛΛ contribution to the potential energy of ${}^{18}_{\Lambda\Lambda}$O.

Some of the conclusions of Ref. [1] were, first, that the NSC89 formalism still relied too heavily on the large ΛN-ΣN tensor coupling. This produced a ${}^{5}_{\Lambda}$He binding energy which was too weak, and any efforts to correct this destroyed agreement with the scattering data. Second, if a fit was forced to the bound state data, the scattering χ^2 would, at best, double. Third, the construction of a *BB* potential is an ongoing process. The paucity of scattering data requires that one make comparisons with hypernuclear properties to see what deficiencies appear and how they may be overcome in the next interaction of the *BB* potential development.

This paper presents the first calculation of Λ binding energies with the potentials of Ref. [1]. The purpose of this calculation is fourfold. The first is to perform large model space Brueckner calculations for ${}^{5}_{\Lambda}$He and ${}^{17}_{\Lambda}$O$(1/2^{+},1/2^{-},3/2^{-})$ and to compare these results with the truncated calculations used in the fits of Ref. [1]. Truncated calculations were employed to provide the speed required for inclusion in a fit, however, their accuracy must be tested. The second is to compare the more accurate calculations with experimental results. The third is to test whether the different potentials developed in Ref. [1] have different predictions in heavier systems. The fourth is to demonstrate some of the dynamics of the ΛN-ΣN coupling and its effect on the single-particle energies.

II. CALCULATION

The calculation proceeds as in Ref. [4], which may be seen for more details. The primary ingredients are as follows. The diagonal Λ single-particle potential for hole states is of Hartree form

$$\langle\Lambda|U|\Lambda\rangle=\sum_{N}\ \langle\Lambda N|g(\omega=\epsilon_{\Lambda}+\epsilon_{N})|\Lambda N\rangle. \tag{2.1}$$

The particle-hole single-particle potential is defined as

$$\langle\Lambda|U|\lambda\rangle=\sum_{N}\ \langle\Lambda N|g(\omega=\epsilon_{\Lambda}+\epsilon_{N})|\lambda N\rangle, \tag{2.2}$$

thereby causing the second-order diagrams in Fig. 1 to cancel. The state $|\lambda\rangle$ could be an excited Λ or Σ state. The particle-particle, single-particle potential is defined in analogy with the Hartree definition of the hole-hole potential

$$\langle\lambda|U|\lambda\rangle=\sum_{N}\ \langle\lambda N|g(\omega=\epsilon_{\lambda}+\epsilon_{N}|\lambda N\rangle. \tag{2.3}$$

The single-particle energy is the single-particle potential plus the kinetic energy,

$$\epsilon_{\Lambda}=\langle\Lambda|T|\Lambda\rangle+\langle\Lambda|U|\Lambda\rangle. \tag{2.4}$$

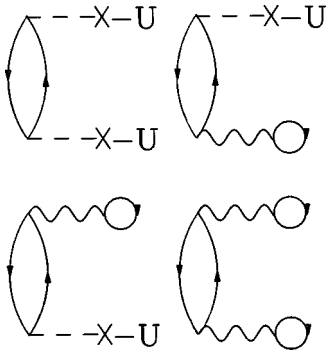

FIG. 1. Second-order diagrams canceled by the definition of the single-particle potential.

The propagator defining the g-matrix element is taken to be

$$\frac{Q}{\omega - Q(T_Y + T_N + \Delta mc^2 \delta_{Y\Sigma})Q}, \tag{2.5}$$

where Q is the Pauli operator, ω is the starting energy, T_Y operates on the coordinates of the hyperon, and T_N operates on the coordinates of the nucleon. The use of the QTQ propagator means that $-U$ insertions are included in particle lines. The reference spectrum g-matrix elements are calculated with the propagator

$$\frac{1}{\omega - (\epsilon_{NL}/2 + T_r + \Delta mc^2 \delta_{Y\Sigma})}, \tag{2.6}$$

where T_r is the relative kinetic energy operator and ϵ_{NL} is $\hbar\Omega(2N+L+3/2)$, assumed to be diagonal in N and L. The term ϵ_{NL} is taken to be $\hbar\Omega(2N+L+3/2)$ even when the intermediate state is a Σ. The reference spectrum g-matrix elements are then corrected to correspond to the propagator in Eq. (2.5) by solving the matrix equation

$$g = g_r + g_r(Q/e - 1/e_r)g. \tag{2.7}$$

An approximation to this equation is

$$g = g_r + g_r[(Q-1)/e_d]g, \tag{2.8}$$

where e_d is $\omega - (T_Y + T_N + \Delta mc^2 \delta_{Y\Sigma})$, taken to be diagonal in n_N, l_N, n_Y, and l_Y. This approximation proved to be very accurate in nucleons only calculations and was used in Ref. [4] and in Ref. [1]. It will be seen below that it is not as accurate as one would like for ${}^{5}_{\Lambda}$He.

The reference spectrum g-matrix elements are calculated by solving the four-component Bethe-Goldstone equation. Four components are necessary because of the ΛN-ΣN coupling, the tensor force, and the antisymmetric spin-orbit force. Because of the cancellation of the second-order diagrams and because the ΛN potential is half the strength of the NN interaction, one would expect the above prescription in Eq. (2.4) to be accurately identified with the Λ separation energy.

One difficulty that arises is that the oscillator size has been chosen to fit the nuclear charge radius, and, therefore, the corresponding size for the lambda ($b_\Lambda^2 = b_\Lambda^2 m_N/m_\Lambda$) may not give a good approximation to the lambda Hartree wave functions. A solution would be to expand the Λ single-particle wave functions in oscillator wave functions. However, this expansion should be carried out in the Λ-nucleus center of mass system to avoid spurious components. This can be accomplished by the transformation introduced in Ref. [5], provided that the effective interaction is translationally invariant. The relative g-matrix elements defined above depend on the starting energy and the quantum numbers of the two-body center of mass wave function and are inappropriate.

Therefore a Hartree condition correction to the energies calculated with harmonic oscillator wave functions with size parameter fit to the nuclear charge radius is calculated as in Ref. [4]. The g-matrix elements in the relative-center of mass basis are $Q-1$ corrected by the average-angle (Emery-Eden) method, $Q=0$ if $2n+2N+l+L \leqslant N_m$. Then one value of ϵ_{NL} and one value of ω are chosen for all g-matrix elements so as to reproduce the single-particle energies calculated above as closely as possible, and a coordinate space effective interaction is fit to these relative g-matrix elements. This effective interaction is used when the Λ-nucleus relative wave function is expanded in oscillators and the energy minimized. This determines a shift in the single-particle energies due to the minimization which is taken to be the Hartree condition correction. The shift is large enough for ${}^{5}_{\Lambda}$He that the process must be iterated in ω.

TABLE I. $-B_\Lambda$ (MeV).

	Ref. [1]		This work	
	Pot. Ib	Pot. IIa	Pot. Ib	Pot. IIa
${}^{5}_{\Lambda}$He	−1.61	−1.68	−2.23	−2.15
${}^{17}_{\Lambda}$O$(1/2^+)$	−13.82	−13.78	−13.75	−13.55
${}^{17}_{\Lambda}$O$(3/2^-)$	−3.03	−3.08	−2.30	−2.23
${}^{17}_{\Lambda}$O$(1/2^-)$	−2.09	−2.15	−1.52	−1.44

III. RESULTS

The calculated single-particle energies for ${}^{5}_{\Lambda}$He and ${}^{17}_{\Lambda}$O$(1/2^+,1/2^-,3/2^-)$ are shown in Table I and compared with those calculated by the approximate technique of Ref. [1]. The oscillator constants employed are shown in Table II. The calculations in Ref. [1] employed highly truncated model spaces, but introduced parameters so that the calculations reproduced the binding energies of NSC89, determined by more accurate methods of Refs. [4] and [6]. The agreement is good enough to show that the inclusion of the truncated calculations in Ref. [1] provided reliable constraints. The truncated calculations could be improved, however, since the approximation in Eq. (2.8) was used in Ref. [4] and is not as accurate as expected for ${}^{5}_{\Lambda}$He. That is the major source of the 0.5 MeV discrepancy between the ${}^{5}_{\Lambda}$He energy in the first two columns and the last two columns. For the p states of ${}^{17}_{\Lambda}$O such a discrepancy is less significant since the experimental energies have large uncertainties, but for ${}^{5}_{\Lambda}$He the B_Λ value of 3.1 MeV is known quite accurately. In future potential parameter fits, the value of the parameter Δ in Table III of Ref. [1] should be changed from 0 to −0.5 MeV.

The final calculated B_Λ values of 2.15 and 2.23 MeV for ${}^{5}_{\Lambda}$He are still too small as compared to experiment. This means that, although some improvement has been made over the original NSC89, the ΛN-ΣN tensor force remains too strong and this part of the force should be scrutinized carefully in the next round of potential development.

The final single-particle energies for ${}^{5}_{\Lambda}$He and ${}^{17}_{\Lambda}$O$(1/2^+,1/2^-,3/2^-)$ as well as ${}^{13}_{\Lambda}$C (taken to be a closed

TABLE II. Oscillator constants b (fm).

${}^{5}_{\Lambda}$He	${}^{13}_{\Lambda}$C	${}^{17}_{\Lambda}$O	${}^{41}_{\Lambda}$Ca	${}^{49}_{\Lambda}$Ca	${}^{91}_{\Lambda}$Zr	${}^{208}_{\Lambda}$Pb
1.394	1.664	1.793	1.970	1.970	2.205	2.516

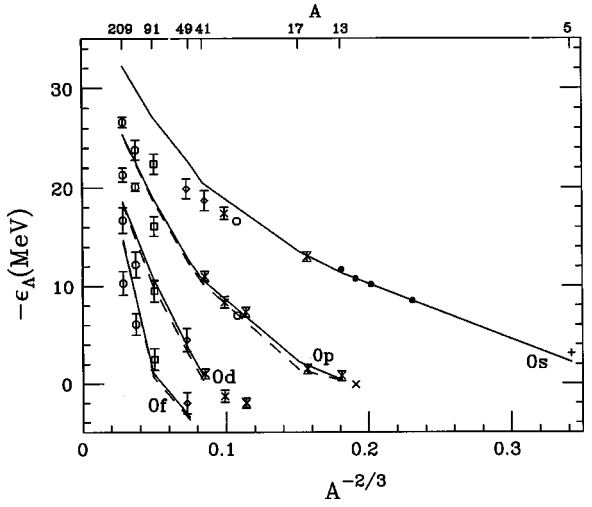

FIG. 2. Calculated single-particle energies including Hartree correction are connected with straight lines. The $j=l-\frac{1}{2}$ states are connected with dashed lines and the $j=l+\frac{1}{2}$ with solid lines. Data are from Refs. [7–12].

$0p_{3/2}$ shell) are plotted in Fig. 2 and connected with straight lines. The $j=l-\frac{1}{2}$ states are connected with dashed lines and the $j=l+\frac{1}{2}$ with solid lines. The calculations shown are for potential IIa of Ref. [1]. The experimental points of Refs. [7–12] are included. One can see that through the $0p$-shell the agreement is quite good. The discrepancy for ${}^{5}_{\Lambda}$He is understood as described above.

It is desirable to extend these calculations to heavier systems. This allows one to investigate the influence of the ΛN-ΣN coupling and to determine whether the different potentials predict different single-particle energies in the heavier systems. It is computationally reasonable to perform calculations for $A=5$ through 91 with the Pauli corrections performed in the appropriate space of wave functions $|n_1 l_1 j_1(\mathbf{r}_Y) n_2 l_2 j_2(\mathbf{r}_N)(J)\rangle$. For this mass range the space can be truncated at $2n_1+l_1+2n_2+l_2 \leqslant N_l$, where $N_l=10$ and the n_i start at zero. This was barely sufficient for $A=91$, and would be very much insufficient for $A=209$. However, Table III demonstrates that performing the Pauli corrections in the relative-center of mass basis, $|nl(\mathbf{r}_{YN})S(j)NL(\mathbf{R})(J)\rangle$, via the average-angle technique is a reasonably good approximation. With $N_m=4$ for ${}^{41}_{\Lambda}$Ca and $N_m=6$ for ${}^{91}_{\Lambda}$Zr one sees a slight tendency for the average-angle Q to overbind. Therefore one would expect to have a good approximation for ${}^{208}_{\Lambda}$Pb with $N_m=10$.

TABLE III. $-B_\Lambda$ (MeV).

	${}^{41}_{\Lambda}$Ca		${}^{91}_{\Lambda}$Zr	
Orbit	Full Q	Average Angle	Full Q	Average Angle
$0s_{1/2}$	−18.80	−19.02	−24.94	−25.05
$0p_{3/2}$	−9.11	−9.75	−17.44	−17.58
$0p_{1/2}$	−8.54	−9.10	−17.20	−17.33
$0d_{5/2}$	0.42	−0.04	−9.66	−10.13
$1s_{1/2}$	1.50	1.05	−8.82	−9.20
$0d_{3/2}$	1.49	1.00	−9.35	−9.79
$0f_{7/2}$			−1.77	−2.32
$0f_{5/2}$			−1.38	−1.84
$1p_{3/2}$			−0.67	−1.10
$1p_{1/2}$			−0.44	−0.86

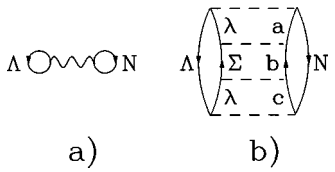

FIG. 3. (a) The first order diagram. (b) The first order diagram expanded to show intermediate states.

Calculations were run for both potentials Ib and IIa of Ref. [1] for ${}^{5}_{\Lambda}$He, ${}^{13}_{\Lambda}$C, ${}^{17}_{\Lambda}$O, ${}^{41}_{\Lambda}$Ca, ${}^{49}_{\Lambda}$Ca, ${}^{91}_{\Lambda}$Zr, and ${}^{208}_{\Lambda}$Pb as described above. The nucleon single-particle energies were taken from experiment where available and from the neutron values of the relativistic Hartree Fock calculation of Ref. [13]. Potential Ib was characterized by having four different momentum cutoff values in $S=-1$ sector, whereas IIa had only one, as determined in the *NN* fit. One might expect that, although their predictions for light systems are similar as shown in Table I, they may have different predictions in heavy systems. This proves to be incorrect. The results for both Ib and IIa remains similar throughout the range of *A*, with potential Ib giving results that are between 0.2 and 0.3 MeV more bound. This is encouraging for efforts to include bound state data in *BB* potential fits, since it appears that one need only include data up to $A=17$ as was done in Ref. [1].

By having the binding energy calculations available over a wide mass range, one can also investigate some of the dynamics of the ΛN-ΣN coupling. First of all, this coupling remains responsible for a huge amount of the Λ binding energy, just as it did for NSC89; and, as in the NSC89 case, this coupling effect is almost entirely in the triplet even channels. In fact, if this coupling is omitted from the reference spectrum *g*-matrix calculations, the ${}^{17}_{\Lambda}$O states become 10 MeV less bound. This corresponds to omitting all intermediate states which include a sigma and a nucleon. Such a state is labeled as $|\Sigma b\rangle$ in the expanded first order diagram in Fig. 3(b).

Second, the spread between single-particle levels in a given hypernucleus and between different hypernuclei is very dependent on this coupling. The effect of the ΛN-ΣN coupling on the single-particle energies can be demonstrated by repeating a calculation in Ref. [4] where successive increases are made to the nucleon Fermi energy for the ΣN pairs in a calculation of the single-particle energies of ${}^{17}_{\Lambda}$O. The Fermi energy for ΛN pairs remains fixed at the ${}^{17}_{\Lambda}$O value. The single-particle energies are calculated first with all ΣN pairs allowed, then with a ${}^{5}_{\Lambda}$He Fermi level, then for ${}^{17}_{\Lambda}$O, and finally with a ${}^{41}_{\Lambda}$Ca Fermi level. Again with reference to Fig. 3(b), one is successively excluding more and more of the intermediate ΣN pairs as the nucleon Fermi energy is increased. When the ΛN-ΣN coupling is strong, the elimination of a set of ΣN pairs has a large effect. The

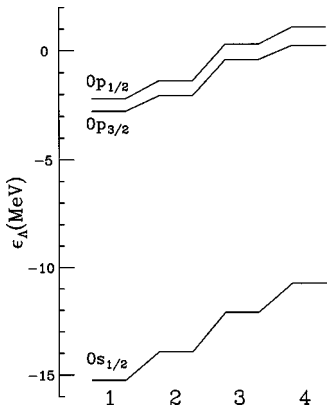

FIG. 4. The single-particle energies of $^{17}_{\Lambda}$O with no Hartree correction. Columns 1, 2, 3, and 4 are for calculations with all ΣN pairs allowed, then with $^{5}_{\Lambda}$He, $^{17}_{\Lambda}$O, and $^{41}_{\Lambda}$Ca Fermi levels.

levels rise and compress as in Fig. 4. If the ΛN-ΣN coupling were small, one would see very little effect.

Third, it is interesting to compare these calculations to those which omit the Σ channels and include their effects via a three-body ΛNN interaction. A very thorough calculation of this type is described in Ref. [14]. If one omits the Σ channels when fitting the ΛN scattering data, the resulting ΛN potential is an effective potential of the form

$$\nu_{\Lambda N}^{\rm eff} = \nu_{\Lambda N} + \nu_{\Lambda\Sigma}\,\frac{P}{E - PTP - \nu_{\Sigma N}}\,\nu_{\Sigma\Lambda}\,, \qquad (3.1)$$

where P allows ΣN states. This effective potential can yield a density dependent effective interaction by placing a Λ in symmetric nuclear matter. This can account for some of the effects of the dependence on the starting energy and the ΛN Fermi energy. However, when imbedded in a nucleus, not all intermediate ΣN pairs are allowed. Some correction to the two-body contribution in Fig. 5(b) must be made. This can be accomplished by introducing an additional interaction which must be density dependent or three-body. Figure 4 demonstrates why this must be so. The $0s$ state is affected more by elimination of successive ΣN pairs than the $0p$ states. This is because reference spectrum g-matrix elements for states closer to the Fermi surface receive a smaller correction. In Ref. [14] the choice was made to employ a three-body interaction. In addition, the diagram in Fig. 5(a) can contribute in the nucleus. Such diagrams are canceled by the choice of the single-particle potential in this work, but are included in Ref. [14] by multiplying the dispersive correction by a density dependent term. Therefore, the effect of omitting Σ channels is taken into account by a density dependent, three-body interaction.

Because of the cancellation of second order diagrams in this work, the approximate size of the contribution of an effective three-body potential can be extracted from a g-matrix calculation by comparing results in which no ΣN pairs are eliminated from intermediate states and results in which the correct ΣN pairs are eliminated. This comparison is made for the single-particle energies with no Hartree correction in Fig. 6, where the solid lines correspond to eliminating the correct ΣN pairs and the dashed lines correspond to eliminating none. One can see that the effect is large over the entire mass range, going from 3 MeV in the $^{5}_{\Lambda}$He ground state to 6 MeV in the $^{208}_{\Lambda}$Pb ground state. Also, one can see that the effect decreases as one goes to higher-lying orbits, thus the necessity of a density dependent or three-body effective interaction, or both. Although the connection is less clear, this difference can also be compared to the ρ^{γ} contribution in potential calculations such as Ref. [15].

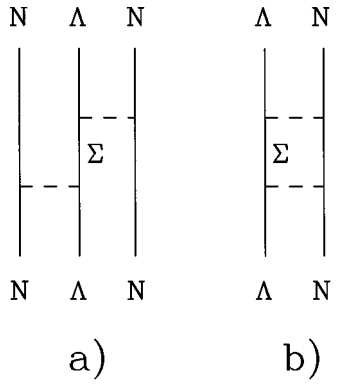

FIG. 5. (a) A three-body contribution. (b) A two-body contribution.

It is with some trepidation that the Hartree corrections are extended to the higher mass nuclei. The procedure was designed for light nuclei for which the harmonic oscillator wave functions provide a good description of the nuclear density. The fear is that some reader will interpret Fig. 2 as the final g-matrix predictions for all systems instead of those in the $0s$ and $0p$ shells. In Fig. 7 are plotted the harmonic oscillator nuclear densities and the charge densities extracted from electron scattering [16] for ^{40}Ca and ^{208}Pb. The great differences in the shapes demonstrates one reason why the predictions for the higher mass nuclei cannot be considered as final. In addition, it becomes much more difficult in the heavy systems to fit the full calculation with one effective

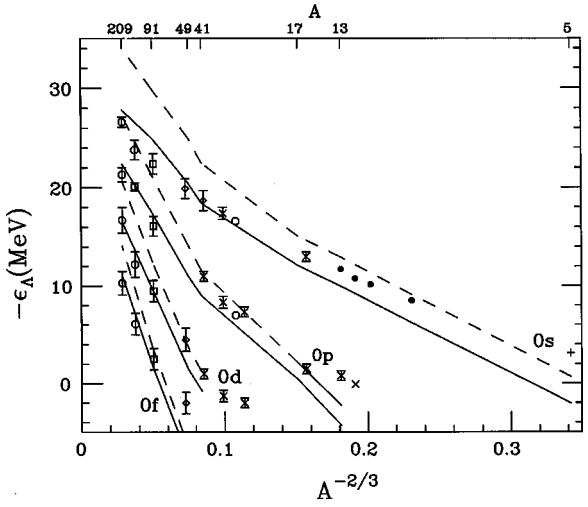

FIG. 6. Solid lines are single-particle energies with proper ΣN pairs eliminated from intermediate states. Dashed lines are with no ΣN pairs eliminated. Data are from Refs. [7–12].

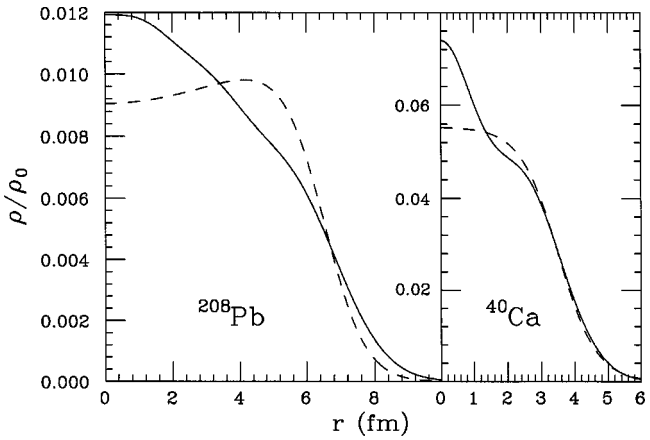

FIG. 7. Oscillator densities are plotted as solid lines. Proton densities extracted from electron scattering are dashed lines.

interaction. Whereas one is introducing uncertainties due to construction of the effective interaction of the order of 0.2 to 0.3 MeV in the light systems, the uncertainties in the heavier systems are of the order of 1.0 to 2.0 MeV. Finally, the work described above assumed that isospin was a good quantum number and did not take into account the difference between the Λp and Λn interactions. Doing so would make the single-particle energies in the heavy systems less bound. However, given the above caveats, Fig. 1 demonstrates an interesting phenomena in that as spin-orbit partners become more deeply bound, the spin-orbit splitting decreases. This is good news for people who locate the positions of major Λ shells via (π, K) data, since the spin-orbit splitting should not contribute to the spread of single-particle strength for deeply bound orbits.

IV. CONCLUSION

This paper has presented calculations of Λ binding energies with the potentials of Ref. [1]. First order Brueckner-Hartree calculations were performed with potentials Ib and IIa for ${}^{5}_{\Lambda}$He, ${}^{13}_{\Lambda}$C, ${}^{17}_{\Lambda}$O, ${}^{41}_{\Lambda}$Ca, ${}^{49}_{\Lambda}$Ca, ${}^{91}_{\Lambda}$Zr, and ${}^{208}_{\Lambda}$Pb. Despite having very different form factor cutoff values in the $S=-1$ sector, results for the two potentials differed little over the $A=5$ to 209 mass range. The results for ${}^{5}_{\Lambda}$He and ${}^{17}_{\Lambda}$O$(1/2^{+},1/2^{-},3/2^{-})$ were within 0.7 MeV of the approximate calculations in Ref. [1]. This shows that the inclusion of the approximate binding energy calculations in potential parameter fits will provide reliable constraints. The $0p$-shell hypernuclei were in good agreement with experimental results, however, ${}^{5}_{\Lambda}$He was underbound by 0.9 and 1.0 MeV for the two potentials. This indicated that the ΛN-ΣN tensor force is too strong as it was in the original NSC89. An estimate of the size of the ΛNN force required in calculations

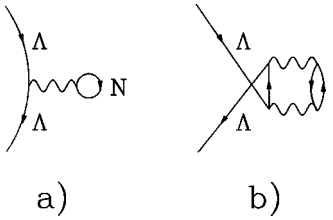

FIG. 8. (a) Diagram for Hartree definition of single-particle energy. (b) An additional possible insertion in a hole line.

which do not include the Σ channels indicated the ΛNN contribution should be between 3 and 6 MeV repulsive for ground states with diminishing importance as the single-particle states approach the Fermi surface.

Finally, it will be important at some stage in the development of *BB* potentials to implement *g*-matrix calculations which are more appropriate for the heavy systems. It would be very interesting to look for small deviations from the experimental single-particle values to see whether an additional mechanism beside the ΣN coupling is at work. This could be due to effects such as quark antisymmetrization [17,18] or partial deconfinement of strange quarks [19].

One cannot make an accurate calculation by extracting a density dependent interaction from nuclear matter calculations and using a local density approximation. This assumes your density dependence can emulate the Fermi energy dependence of both ΛN and ΣN pairs, starting energy dependence, the two-particle center of mass dependence, and the difference between the proton and neutron Fermi energies. Although it may not be necessary to work in the Λ-nucleus center of mass system for heavy nuclei, it will still be necessary to expand the Λ wave function in oscillators. It will also be necessary to employ realistic nuclear wave functions, expressed as an expansion of oscillator wave functions.

One may also want to look at higher order corrections to the single-particle energies. In addition to the diagram in Fig. 8(a), which represents Eq. (2.1), one can make other insertions in Λ hole lines, such as Fig. 8(b). In fact, one can make an arbitrary number of such insertions, which leads to the concept of partial occupation probabilities (POP) for which each matrix element in Eq. (2.1) is multiplied by the corresponding nucleon POP [20,21]. Such terms were included in one of the first Brueckner calculations for light hypernuclei [22]. However, for the heavy systems, special care must be given to the self-consistency of the wave functions and calculation of the diagrams.

ACKNOWLEDGMENT

This work was supported by the National Science Foundation under Grant No. PHY-9732634.

[1] D. Halderson, Phys. Rev. C **60**, 064001 (1999).
[2] M. M. Nagels, T. A. Rijken, and J. J. de Swart, Phys. Rev. D **17**, 768 (1978).
[3] P. M. M. Maessen, Th. A. Rijken, and J. J. de Swart, Phys. Rev. C **40**, 2226 (1989).
[4] D. Halderson, Phys. Rev. C **48**, 581 (1993).
[5] D. Halderson, Phys. Rev. C **30**, 941 (1984).
[6] J. A. Carlson, *Proceedings of the LAMPF Workshop on (π, K) Physics*, AIP Conf. Proc. No. 224, edited by B. F. Gibson, W. R. Gibbs, and M. B. Johnson (AIP, New York, 1991), p. 198.

[7] P. H. Pile *et al.*, Phys. Rev. Lett. **66**, 2585 (1991).
[8] T. Hasegawa *et al.*, Phys. Rev. C **53**, 1210 (1996).
[9] R. Chrien, Nucl. Phys. **A478**, 705c (1988).
[10] C. Milner *et al.*, Phys. Rev. Lett. **54**, 1237 (1985).
[11] R. Bertini *et al.*, Phys. Lett. **83B**, 306 (1979).
[12] R. Bertini *et al.*, Nucl. Phys. **A360**, 315 (1981).
[13] M. Chiapparini, A. Delfino, M. Matheiro, and A. Gattone, Z. Phys. A **357**, 47 (1997).
[14] Q. N. Usmani and A. R. Bodmer, Nucl. Phys. **A639**, 147c (1998).
[15] D. J. Millener, C. B. Dover, and A. Gal, Phys. Rev. C **38**, 2700 (1988).
[16] C. W. De Jager, H. De Vries, and C. De Vries, At. Data Nucl. Data Tables **14**, 47899 (1974).
[17] S. Takeuchi and K. Shimizu, Phys. Lett. B **179**, 197 (1986).
[18] E. V. Hungerford and L. C. Biedenharn, Phys. Lett. **142B**, 232 (1984).
[19] T. Goldman, *Intersections Between Particle and Nuclear Physics*, AIP Conf. Proc. No. 123, edited by R. E. Mischke (AIP, New York, 1984), p. 799.
[20] B. H. Brandow, *Lectures in Theoretical Physics*, edited by K. T. Mahanthappa and W. E. Brittin (Gordon and Breach, New York, 1969), Vol. XI-B.
[21] R. L. Becker, Phys. Rev. Lett. **24**, 400 (1970).
[22] Y. Yamamoto and H. Bando, Suppl. Prog. Theor. Phys. **81**, 9 (1985).